VOLUME 112, NUMBER 19
SEPTEMBER 12, 1990

JOURNAL
OF THE
AMERICAN
CHEMICAL
SOCIETY

Theoretical Study of H_2 Elimination from B_4H_{10}, B_5H_{11}, and B_6H_{12} and BH_3 Elimination from B_4H_{10}[†]

Michael L. McKee

Contribution from the Department of Chemistry, Auburn University, Auburn, Alabama 36849-5312. *Received August 24, 1989*

Abstract: Ab initio calculations are employed to evaluate decomposition pathways of several boron hydrides. Reactants, products, and transition states for the decomposition of B_4H_{10} were optimized at the MP2/6-31G* level. The predicted barrier for formation of $B_4H_8 + H_2$ is in good agreement with experiment (26.8 (calcd) and 23.7 (exptl) kcal/mol) while the barrier for formation of $B_3H_7 + BH_3$ is 13.7 kcal/mol higher. Loss of H_2 from B_5H_{11} and B_6H_{12} is predicted to occur with activation barriers of 52.8 and 37.4 kcal/mol, respectively (MP2/6-31G*//3-21G). The most significant discovery is that the observed decomposition of B_5H_{11} cannot occur as previously thought by the reaction $B_5H_{11} \rightarrow B_4H_8 + BH_3$ since this reaction has a calculated endothermicity 18.1 kcal/mol *greater* than the observed activation barrier.

Introduction

While the thermal reactions of the boron hydrides have received much experimental attention,[1-8] relatively few theoretical studies have appeared. The exception is the dimerization of BH_3 to form B_2H_6, which has served as a benchmark for high-level calculations.[9-13] Calculations at the Hartree–Fock level predict dimerization energies about one-half of that observed. This system is therefore a good test for post-SCF methods.

Two unimolecular decomposition pathways can be written for the smaller boron hydrides B_4H_{10} (eq 1), B_5H_{11} (eq 2), and B_6H_{12} (eq 3). The first pathway eliminates molecular hydrogen while

$$B_4H_{10} \rightarrow B_4H_8 + H_2 \quad (1a)$$

$$B_4H_{10} \rightarrow B_3H_7 + BH_3 \quad (1b)$$

$$B_5H_{11} \rightarrow B_5H_9 + H_2 \quad (2a)$$

$$B_5H_{11} \rightarrow B_4H_8 + BH_3 \quad (2b)$$

$$B_6H_{12} \rightarrow B_6H_{10} + H_2 \quad (3a)$$

$$B_6H_{12} \rightarrow B_5H_9 + BH_3 \quad (3b)$$

the second produces BH_3. Both pathways produce a borane that can further react, making it difficult to isolate one boron hydride reaction for study. In the pyrolysis of B_2H_6, the rate-determining step is usually considered to be the elimination of H_2 from B_3H_9 (eq 4a) rather than the addition of BH_3 to B_2H_6 (eq 4b).[1,2]

$$B_3H_9 \rightarrow B_3H_7 + H_2 \quad (4a)$$

$$B_2H_6 + BH_3 \rightarrow B_3H_9 \quad (4b)$$

[†] Dedicated to Professor William N. Lipscomb on the occasion of his 70th birthday.

(1) (a) Greenwood, N. N.; Greatrex, R. *Pure Appl. Chem.* **1987**, *59*, 857–868. (b) Gibbs, T. C.; Greenwood, N. N.; Spalding, T. R.; Taylorson, D. *J. Chem. Soc., Dalton Trans.* **1979**, 1392–1397.
(2) Fehlner, T. P. In *Boron Hydride Chemistry*; Mutterties, E. L., Ed.; Academic Press: New York, 1975; pp 175–196.
(3) Greatrex, R.; Greenwood, N. N.; Lucas, S. M. *J. Am. Chem. Soc.* **1989**, *111*, 8721–8722.
(4) Greatrex, R.; Greenwood, N. N.; Potter, C. D. *J. Chem. Soc., Dalton Trans.* **1984**, 2435–2437.
(5) Attwood, M. D.; Greatrex, R.; Greenwood, N. N. *J. Chem. Soc., Dalton Trans.* **1989**, 385–390.
(6) Attwood, M. D.; Greatrex, R.; Greenwood, N. N. *J. Chem. Soc., Dalton Trans.* **1989**, 391–397.
(7) Greatrex, R.; Greenwood, N. N.; Jump, G. A. *J. Chem. Soc., Dalton Trans.* **1985**, 541–548.
(8) Greatrex, R.; Greenwood, N. N.; Waterworth, S. D. *J. Chem. Soc., Chem. Commun.* **1988**, 925–926.
(9) Page, M.; Adams, G. F.; Binkley, J. S.; Melius, C. F. *J. Phys. Chem.* **1987**, *91*, 2675.
(10) Curtiss, L. A.; Pople, J. A. *J. Chem. Phys.* **1988**, *89*, 4875.
(11) Stanton, J. F.; Bartlett, R. J.; Lipscomb, W. N. *Chem. Phys. Lett.* **1987**, *138*, 525.
(12) Defrees, D. J.; Raghavachari, K.; Schlegel, H. B.; Pople, J. A.; Schleyer, P. v. R. *J. Phys. Chem.* **1987**, *91*, 1857.

0002-7863/90/1512-6753$02.50/0

Table I. Absolute Energies (hartrees) of Various Species

		//3-21G				//6-31G*			
	symm	3-21G	6-31G*	MP2/6-31G*	ZPE[a]	6-31G*	MP2/6-31G*	MP4/6-31G*	ZPE[a]
H_2	$D_{\infty h}$	-1.12296	-1.12681	-1.14414	6.66 (0)	-1.12683	-1.14410	-1.15082	6.64 (0)
BH_3	D_{3h}	-26.23730	-26.39001	-26.46422	17.29 (0)	-26.39001	-26.46423	-26.48324	17.38 (0)
B_2H_6	D_{2d}	-52.49781	-52.81237	-52.99241	41.77 (0)	-52.81240	-52.99259	-53.03092	41.89 (0)
B_3H_7	C_s	-77.58501	-78.04734	-78.31355	49.46 (0)	-78.04764	-78.31451	-78.36592	50.14 (0)
B_3H_9	C_{3v}	-78.71778	-79.18208	-79.45889	62.44 (0)	-79.18352	-79.46481	-79.52293	63.68 (0)
B_4H_8	C_1					-103.29667	-103.66224	-103.72517	59.01 (0)
B_4H_8	C_2	-102.68689	-103.29433	-103.65251	58.21 (0)	-103.29164	-103.65650	-103.71998	58.63 (0)
B_4H_8	C_s	-102.69517	-103.29747	-103.64944	58.12 (0)	-103.29816	-103.65174	-103.71603	58.27 (0)
B_4H_8	C_{2v}	-102.66811	-103.27972	-103.64930	55.35 (3)	-103.28059	-103.65168	-103.71438	56.11 (3)
B_4H_8 (2)	C_{2v}	-102.65962	-103.27292	-103.64521	58.25 (0)	-103.27341	-103.64657	-103.70835	59.20 (0)
B_4H_{10}	C_{2v}	-103.84390	-104.45676	-104.84052	72.83 (0)	-104.45702	-104.84134	-104.90927	73.16 (0)
$B_3H_7 + H_2$	C_1	-78.67245	-79.13864	-79.44287	60.99 (1)	-79.13860	-79.44310	-79.49860	61.46 (1)
$B_4H_8 + H_2$	C_s	-103.79184	-104.39978	-104.77755	69.11 (1)	-104.40014	-104.77758	-104.84740	69.56 (1)
$B_4H_8 + H_2$	C_1	-103.78184	-104.39142	-104.78129	69.92 (1)	-104.39155	-104.78139	-104.84913	70.48 (1)
B_5H_9	C_{4v}	-127.82196	-128.57807	-129.04858	69.50 (0)				
B_5H_{11}	C_1	-128.94960	-129.71016	-130.18378	81.38 (0)				
B_6H_{10}	C_s	-152.93910	-153.83762	-154.39702	79.32 (0)				
B_6H_{12}	C_2	-154.06351	-154.97197	-155.53791	91.63 (0)				
$B_5H_9 + H_2$	C_1	-128.87845	-129.62865	-130.09528	77.29 (1)				
$B_6H_{10} + H_2$	C_1	-153.99319	-154.89508	-155.47465	88.69 (1)				
$B_4H_8 + BH_3$	C_1	-128.87904	-129.63789	-130.09668					

[a] Zero-point energy (kcal/mol). Number of imaginary frequencies is given in parentheses.

Table II. Absolute Energies (hartrees) for Various Species at MP2/6-31G* Optimized Geometries

		//MP2/6-31G*				
	symm	6-31G*	MP2/6-31G*	MP4/6-31G*	6-311G**	MP2/6-311G**
H_2	$D_{\infty h}$	-1.12679	-1.14414	-1.14933	-1.13249	-1.16027
BH_3	D_{3h}	-26.39000	-26.46424	-26.48329	-26.39698	-26.49466
B_2H_6	D_{2d}	-52.81213	-52.99281	-53.03114	-52.82757	-53.05639
B_3H_7	C_s	-78.04661	-78.31542	-78.36679	-78.06688	-78.39291
B_3H_9	C_{3v}	-79.17612	-78.47054	-79.52778	-79.20106	-79.56766
B_4H_8	C_1	-103.29514	-103.66397	-103.72644	-103.32114	-103.75664
B_4H_8[a]	C_2	-103.21362	-103.65658	-103.72004	-103.31685	-103.74885
B_4H_8	C_s	-103.29272	-103.65510	-103.71863	-103.31858	-103.74801
B_4H_8	C_{2v}	-103.27921	-103.65296	-103.71513	-103.30668	-103.74715
B_4H_8 (2)	C_{2v}	-103.26998	-103.64960	-103.71071	-103.29648	-103.74311
B_4H_{10}	C_{2v}	-104.45444	-104.84356	-104.91095	-104.48269	-104.95409
$B_3H_7 + BH_3$	C_1	-104.40666	-104.77125	-104.84207	-104.43535	-104.88462
$B_4H_8 + H_2$	C_s	-104.39960	-104.77749	-104.84764	-104.43276	-104.89158

[a] The molecule was optimized within C_1 symmetry; however, the coordinates are very close to C_2 symmetry.

However, in a recent theoretical study Stanton, Lipscomb, and Bartlett have presented computational evidence[14] that the reaction may proceed directly from B_2H_6 plus BH_3 to B_3H_7 plus H_2. Very recent experimental work[3] with a mass spectrometric technique confirms the theoretical prediction and indicates that the rate-determining step is neither formation of B_3H_9 from BH_3 and B_2H_6 nor elimination of H_2 from B_3H_9 to give B_3H_7 but rather the concerted formation of B_3H_7 plus H_2 from BH_3 and B_2H_6.

Method

All calculations were carried out by using the GAUSSIAN 86 and GAUSSIAN 88 program packages.[15] Geometries were fully optimized within the appropriate point group at the HF/3-21G, HF/6-31G*, and MP2/6-31G* levels. Vibrational frequencies were calculated at the HF/3-21G and HF/6-31G* levels in order to make zero-point and heat capacity corrections. The zero-point energies were weighted by a factor of 0.9 to compensate for systematic overestimation of vibrational frequencies at the HF/3-21G and HF/6-31G* levels.[16] Enthalpies were corrected to 400 K by including heat capacity corrections[17] in order to estimate enthalpies at pyrolysis conditions (40–150 °C). Tables I and II contain total energies at various levels for geometries optimized at the HF/3-21G and HF/6-31G* levels (Table I) and at the MP2/6-31G* level (Table II). Figure 1 contains selected geometric parameters optimized at the MP2/6-31G* level while computer-generated internal coordinates are available as supplementary material. Optimized geometries of B_3H_9,[18] B_4H_8,[19] B_5H_9,[20] B_5H_{11},[21] B_6H_{10},[21] and B_6H_{12}[22] at the HF/3-21G level have been previously reported. In addition optimized geometries of B_3H_7[14] and B_3H_9[14,23] have been reported with a double-ζ plus polarization basis set including electron correlation at the MP2 level of theory.

Forward and reverse activation barriers as well as heats of reaction are given in Table III for the pyrolysis reactions considered. Heats of reaction for boron hydrides forming BH_3 are given in Table IV. The highest level calculations were at the MP2/6-31G* level for 3-21G ge-

(13) Sana, M.; Leroy, G.; Henriet, Ch. *THEOCHEM* **1989**, *187*, 233.
(14) Stanton, J. F.; Lipscomb, W. N.; Bartlett, R. J. *J. Am. Chem. Soc.* **1989**, *111*, 5165–5173.
(15) (a) GAUSSIAN 86: Frisch, M. J.; Binkley, J. S.; Schlegel, H. B.; Raghavachari, K.; Melius, C. F.; Martin, R. L.; Stewart, J. J. P.; Bobrowicz, F. W.; Rohlfing, C. M.; Kahn, L. R.; Defrees, D. J.; Seeger, R.; Whiteside, R. A.; Fox, D. J.; Fleuder, E. M.; Pople, J. A. Carnegie-Mellon Quantum Chemistry Publishing Unit, Pittsburgh, PA 1984. (b) GAUSSIAN 88: Frisch, M. J.; Head-Gordon, M.; Schlegel, H. B.; Raghavachari, K.; Binkley, J. S.; Gonzalez, C.; Defrees, D. J.; Fox, D. J.; Whiteside, R. A.; Seeger, R.; Melius, C. F.; Baker, J.; Martin, R. L.; Kahn, L. R.; Stewart, J. J. P.; Fleuder, E. M.; Topiol, S.; Pople, J. A. Carnegie-Mellon Quantum Chemistry Publishing Unit, Pittsburgh, PA.
(16) For a description of basis sets and use of the 0.9 weighing factor for vibrational frequencies see: Hehre, W. J.; Radom, L.; Schleyer, P. v. R.; Pople, J. A. *Ab Initio Molecular Orbital Theory*; Wiley: New York, 1986.
(17) See: McKee, M. L.; Shevlin, P. B.; Rzepa, H. S. *J. Am. Chem. Soc.* **1986**, *108*, 5793.
(18) B_3H_9: McKee, M. L.; Lipscomb, W. N. *Inorg. Chem.* **1985**, *24*, 2317.
(19) B_4H_{10}: McKee, M. L.; Lipscomb, W. N. *Inorg. Chem.* **1981**, *20*, 4452.
(20) B_5H_9: McKee, M. L.; Lipscomb, W. N. *Inorg. Chem.* **1985**, *24*, 765.
(21) McKee, M. L. *J. Phys. Chem.* **1989**, *93*, 3426–3429.
(22) McKee, M. L. *J. Phys. Chem.* **1990**, *94*, 435.
(23) Stanton, J. F.; Lipscomb, W. N.; Bartlett, R. J.; McKee, M. L. *Inorg. Chem.* **1989**, *28*, 109–111.

Table III. Calculated Forward and Reverse Barrier Heights and Heats of Reaction

	$B_2H_6 \rightarrow 2BH_3$	$B_3H_9 \rightarrow B_3H_7 + H_2$			$B_4H_{10} \rightarrow B_3H_7 + BH_3$			$B_4H_{10} \rightarrow B_4H_8^a + H_2$			$B_5H_{11} \rightarrow B_5H_9 + H_2$			$B_6H_{12} \rightarrow B_6H_{10} + H_2$		
	ΔH_r	f	r	ΔH_r	f	r	ΔH_r	f	r	ΔH_r	f	r	ΔH_r	f	r	ΔH_r
							//3-21G									
3-21G	14.6	28.4	22.3	6.1			13.5	32.7	16.5	16.2	44.6	41.7	2.9	44.1	43.2	0.9
6-31G*	20.3	27.2	22.3	4.9			12.2	35.8	15.4	20.4	51.1	47.8	3.3	48.2	43.5	4.7
MP2/6-31G*	40.1	10.0	9.3	0.7			39.4	39.5	10.0	29.5	55.5	61.1	−5.6	39.7	41.7	−2.0
+ZPC/3-21G	33.6	8.7	13.7	−5.0			33.9	36.2	13.9	22.3	51.8	62.1	−10.3	37.1	44.1	−7.0
							//6-31G*									
6-31G*	20.3	28.2	22.5	5.7			12.2	35.7	14.7	21.0						
MP2/6-31G*	40.2	13.6	9.7	3.9			39.3	40.0	18.0	22.0						
MP4/6-31G*	40.4	15.3	11.4	3.9			37.7	38.8	17.9	20.9						
+ZPC/6-31G*	34.0	13.3	15.6	−2.3			32.6	35.6	21.4	14.2						
							//MP2/6-31G*									
MP2/6-31G*	40.9			6.8	45.9	5.0	40.9	41.6	19.5	22.1						
MP4/6-31G*	40.5			7.3	43.2	5.0	38.2	39.7	17.7	22.0						
MP2/6-311G**	42.1			9.1	43.6	1.8	41.8	31.3	15.9	15.4						
[MP4/6-311G**]	41.7			9.6	40.9	1.8	39.1	29.4	14.1	15.3						
+ZPC/6-31G*	35.3			3.4	38.0	2.9	35.1	26.2	17.6	8.6						
C_p correction	4.1	−0.5	−3.8	3.3	2.5	−0.7	3.2	0.6	−3.5	4.5	1.0	−1.5	2.5	0.3	−2.8	3.1
"best"	39.4[b]	12.8	11.8	6.4	40.5	2.2	38.8	26.8	14.1	13.1	52.8	60.6	−7.8[c]	37.4	41.3	−3.9

[a] The B_4H_8 molecule is the C_s structure (double-bridged) at the HF/3-21G level and the C_1 structure (triple-bridged) at the HF/6-31G* and MP2/6-31G* levels. [b] Experimental difference at 298 K is 39.2 kcal/mol [Guest, M. F.; Pedley, J. B.; Horn, M. *J. Chem. Thermodyn.* **1969**, *1*, 345] or 34.3–39.1 kcal/mol [Ruscic, B.; Mayhew, C. A.; Berkowitz, J. *J. Chem. Phys.* **1988**, *88*, 5580]. [c] Experimental difference at 298 K is −6.8 kcal/mol [Guest, et al. *J. Chem. Thermodyn.* **1969**, *1*, 345].

Table IV. Calculated Reaction Energies for Reactions Forming a Boron Hydride plus BH_3

	$B_3H_9 \rightarrow B_2H_6 + BH_3$	$B_4H_{10} \rightarrow B_3H_7 + BH_3$	$B_5H_{11} \rightarrow B_4H_8 + BH_3$	$B_6H_{12} \rightarrow B_5H_9 + BH_3$
MP2/6-31G*//3-21G	1.4	39.4	37.4[a,b]	15.8
MP2/6-31G*//6-31G*	5.0	39.3		
MP4/6-31G*//6-31G*	5.5	37.7		
MP2/6-31G*//MP2/6-31G*	9.0	40.9		
MP4/6-31G*//MP2/6-31G*	8.4	38.2		
MP2/6-311G**//MP2/6-31G*	10.4	41.8		
[MP4/6-311G**//MP2/6-31G*]	9.8	39.1		
+ZPC/(6-31G* or 3-21G)	5.8	35.1	32.7	11.4
C_p correction at 400 K	2.6	3.2	3.3	2.4
"best"	8.4	38.3	36.0	13.8

[a] The B_4H_8 molecule is the C_s structure (double-bridged). The barrier has been reduced by 6.6 kcal/mol which is the triple-bridged (C_1) and double-bridged (C_s) separation at the MP2/6-31G*//6-31G* level. [b] At the MP2/6-311G**//3-21G level the reaction is predicted to be 45.9 kcal/mol endothermic with respect to the C_s structure of B_4H_8. A reduction of 6.6 kcal/mol for the $C_1 - C_s$ energy difference (at the MP2/6-31G*//HF/6-31G* level) would make the heat of reaction 39.3 kcal/mol.

ometries, while for 6-31G* geometries, calculations were carried through the full MP4 level. Larger basis set calculations are carried out on MP2/6-31G* geometries. The effect of calculations at the MP4/6-31G* level and at the MP2/6-311G** level were assumed to be additive, and results at the [MP4/6-311G**] level (brackets are used to indicate that results at this level of theory were not calculated directly but rather estimated by use of the additivity approximation)[24] were determined from eq 5.

$$\Delta E_{[MP4/6\text{-}311G^{**}]} = \Delta E_{(MP4/6\text{-}31G^*)} + \Delta E_{(MP2/6\text{-}311G^{**})} - \Delta E_{(MP2/6\text{-}31G^*)} \quad (5)$$

The effect of geometry optimization is assessed at the MP2/6-31G* and MP4/6-31G* levels in Table V. At the MP2/6-31G* level the lowest energies will clearly be the ones optimized at that level. It is interesting to note the increase in the MP2/6-31G* energy when 6-31G* geometries are used is about half that of 3-21G geometries. The largest increase in energy is for B_3H_9 and B_4H_8, which are higher by 7.3 and 3.6 kcal/mol, respectively, at 3-21G geometries. Since this difference is much larger than for other boron hydrides, the often assumed cancellation of error due to geometry optimization at a lower level of theory will not occur when comparing reactions that include B_3H_9 and B_4H_8. At the MP4/6-31G* level the differences between 6-31G* and MP2/6-31G* geometries are very similar to the difference at the MP2/6-31G* level. The 6-31G* geometry of H_2 is closer to the MP4/6-31G* geometry than is the MP2/6-31G* geometry as shown by the lower MP4/6-31G* energy at this geometry (Table V).

Table V. Relative Energies (kcal/mol) for Species Optimized at Different Levels of Theory

	MP2/6-31G*			MP4/6-31G*	
	//3-21G	//6-31G*	//MP2/6-31G*	//6-31G*	//MP2/6-31G*
H_2	0.0	0.0	0.0	−0.9	0.0
BH_3	0.0	0.0	0.0	0.0	0.0
B_2B_6	0.2	0.1	0.0	0.1	0.0
B_3H_7	1.2	0.6	0.0	0.5	0.0
B_3H_9	7.3	3.6	0.0	3.0	0.0
$B_4H_8(C_1)$	*a*	1.1	0.0	0.8	0.0
$B_4H_8(C_2)$	2.6	0.0	0.0	0.0	0.0
$B_4H_8(C_s)$	3.6[b]	2.1	0.0	1.6	0.0
$B_4H_8(C_{2v})$	2.3	0.8	0.0	0.5	0.0
$B_4H_8(C_{2v})$[c]	2.9	1.9	0.0	1.5	0.0
B_4H_{10}	1.9	1.4	0.0	1.0	0.0
$B_4H_8 + H_2$	0.0	0.0	0.0	0.2	0.0

[a] Not a minimum at the HF/3-21G level. [b] At the MP2/6-311G** level, the //3-21G – //MP2/6-31G* difference for B_4H_8 is 3.4 kcal/mol. [c] Structure **2** (see text).

Results and Discussion

A set of reactions for the pyrolysis of diborane can be written as eq 6–14, where B_4H_{10}, B_5H_9, B_5H_{11}, B_6H_{12}, and B_6H_{10} are stable

(24) (a) McKee, M. L.; Lipscomb, W. N. *J. Am. Chem. Soc.* **1981**, *103*, 4673. (b) Nobes, R. H.; Bouma, W. J.; Radom, L. *Chem. Phys. Lett.* **1982**, *89*, 497. (c) McKee, M. L.; Lipscomb, W. N. *Inorg. Chem.* **1985**, *24*, 762.

$$B_2H_6 \rightarrow 2BH_3 \quad (6)$$

$$B_2H_6 + BH_3 \rightarrow B_3H_9 \quad (7)$$

$$B_3H_9 \rightarrow B_3H_7 + H_2 \quad (8)$$

$$B_3H_7 + B_2H_6 \rightarrow B_4H_{10} + BH_3 \quad (9)$$

$$B_4H_{10} \rightarrow B_4H_8 + H_2 \quad (10)$$

$$B_4H_8 + B_2H_6 \rightarrow B_5H_{11} + BH_3 \quad (11)$$

$$B_5H_{11} \rightarrow B_5H_9 + H_2 \quad (12)$$

$$B_5H_9 + B_2H_6 \rightarrow B_6H_{12} + BH_3 \quad (13)$$

$$B_6H_{12} \rightarrow B_6H_{10} + H_2 \quad (14)$$

boron hydrides that can be observed as the reaction proceeds. The ratio of stable boron hydrides formed in the pyrolysis can be altered by the pyrolysis conditions. For example, the yield of B_4H_{10} can be increased by short pyrolysis times.[25] Longer times result in formation of B_9H_{15} and $B_{10}H_{14}$ for which several reactions can be written.

Reactions 9, 11, and 13 would undoubtedly have lower barriers for the addition of BH_3 rather than B_2H_6, but the very low concentration of BH_3 would make formation of higher boranes by this route negligible. However, the unimolecular decomposition of higher borane hydrides into a smaller boron hydride plus borane may be important (eqs 1b, 2b, 3b). To model the overall mechanism, kinetic parameters are necessary for all important reactions. Unfortunately, very few are available.

As a start in unravelling this complex mechanism, Greatrex, Greenwood, and co-workers[1,4-8] have carried out kinetic studies of thermal reactions of individual boron hydrides as well as studies in which a boron hydride is pyrolyzed in the presence of hydrogen or another boron hydride. Product distributions can be determined as a function of time, and the inhibitory or enhancing effect of an added species can also be studied.

Decomposition of B_4H_{10}. Early literature can be cited as favoring the decomposition of B_4H_{10} via eq 1a[26-32] or eq 1b.[33,34] More recent research, however, supports the elimination of H_2 over the elimination of BH_3 as the favored pathway.[4,6] In particular, mass spectrometric data indicate that there is direct exchange between dideuterium and B_4H_{10} in the gas phase. The results in Table III at the highest level indicate a barrier of 26.8 kcal/mol, which is in good agreement with the experimental barrier of 23.8 kcal/mol.[4,6] The predicted pre-exponential factor is too large by about 2 orders of magnitude (2×10^{13} (calcd) and 6×10^{11} s^{-1} (exptl)[4,6]).

The transition state for elimination of H_2 has been located at all three levels of theory, HF/3-21G, HF/6-31G*, and MP2/6-31G* (Table III). At the MP2/6-31G*//3-21G and MP4/6-31G*//6-31G* levels the predicted barrier is too high by over 10 kcal/mol. A large stabilization of the transition state occurs when a triple-ζ basis on boron and polarization functions on hydrogen are added. The calculated activation barrier at the MP2/6-311G**//MP2/6-31G* level is 10.3 kcal/mol lower than the calculated activation barrier at the MP2/6-31G*//MP2/6-31G* level. The barrier decreases 1.9 kcal/mol when the additivity approximation is applied and a further 3.2 kcal/mol when zero-point corrections are made. Heat capacity corrections increase the activation barrier by 0.6 kcal/mol. This latter correction is overestimated by 0.1 kcal/mol since corrections are made at 400 K while the experimental barrier is determined at 315 K.

The transition state for elmination of hydrogen is very late, as judged by the short H–H distance of 0.751 Å (MP2/6-31G*), and involves the conversion of adjacent hydrogen bridges into a hydrogen molecule. At the HF/3-21G and HF/6-31G* levels a transition state was located for the asymmetric elimination of H_2 (i.e. the conversion of a terminal and bridging hydrogen into H_2). At the HF/3-21G and HF/6-31G* level, the C_1 transition state is only 6.3 and 5.4 kcal/mol higher than the C_s transition

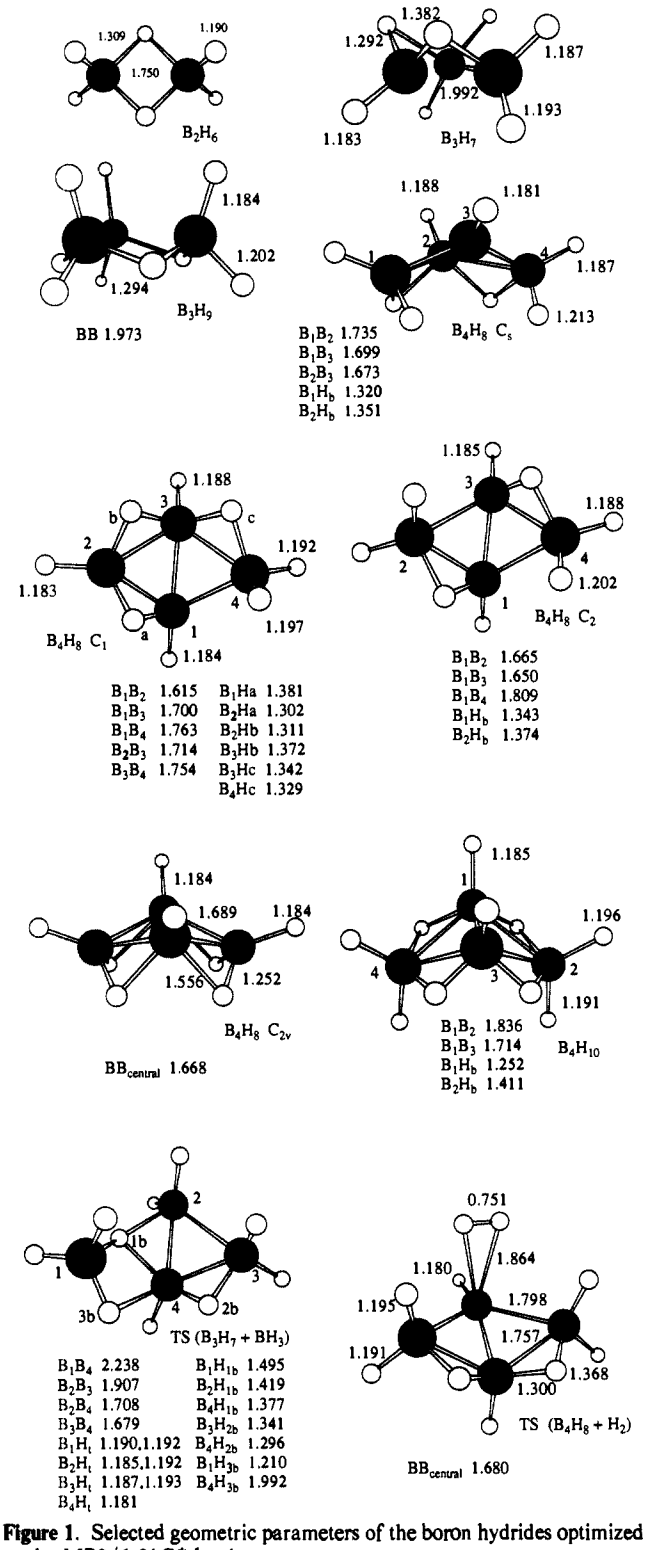

Figure 1. Selected geometric parameters of the boron hydrides optimized at the MP2/6-31G* level.

The transition state for elmination of hydrogen is very late, as judged by the short H–H distance of 0.751 Å (MP2/6-31G*), and involves the conversion of adjacent hydrogen bridges into a hydrogen molecule. At the HF/3-21G and HF/6-31G* levels a transition state was located for the asymmetric elimination of H_2 (i.e. the conversion of a terminal and bridging hydrogen into H_2). At the HF/3-21G and HF/6-31G* level, the C_1 transition state is only 6.3 and 5.4 kcal/mol higher than the C_s transition

(25) Hughes, R. L.; Smith, I. C.; Lawless, E. W. *Production of the Boranes and Related Research*; Holzman, R. T., Ed.; Academic Press: New York, 1967; Chapter 7.
(26) Norman, A. D.; Schaeffer, R. *J. Am. Chem. Soc.* **1966**, *88*, 1143.
(27) Norman, A. D.; Schaeffer, R.; Baylis, A. B.; Pressley, G. A.; Stafford, F. E. *J. Am. Chem. Soc.* **1966**, *88*, 2151.
(28) Schaeffer, R.; Sneddon, L. G. *Inorg. Chem.* **1972**, *11*, 3098.
(29) Baylis, A.; Pressley, G. A.; Gordon, M. E.; Stafford, F. E. *J. Am. Chem. Soc.* **1966**, *88*, 929.
(30) Hollins, R. E.; Stafford, F. E. *Inorg. Chem.* **1970**, *9*, 877.
(31) Stafford, F. E. *Bull. Soc. Chem. Belg.* **1972**, *81*, 81.
(32) Ganguli, P. S.; Gordon, L. P.; McGee, H. A. *J. Chem. Phys.* **1970**, *53*, 782.
(33) Koski, W. S. *Adv. Chem. Ser.* **1961**, *32*, 78.
(34) Bond, A. C.; Pinksy, M. L. *J. Am. Chem. Soc.* **1970**, *92*, 32.

Table VI. Comparison of Theoretical and Experimental Kinetic Parameters for the Decomposition of B_4H_{10}, B_5H_{11}, and B_6H_{12}

	B_4H_{10} decomp[e]		B_5H_{11} decomp[f]			B_6H_{12} decomp[g]	
	$B_4H_{10} \rightarrow B_4H_8 + H_2$	$B_4H_{10} \rightarrow B_3H_7 + BH_3$	$B_5H_{11} \rightarrow B_4H_8$[a] $+ BH_3$	$2B_5H_{11} \rightarrow B_3H_7 + B_5H_9 + B_2H_6$	$B_5H_{11} \rightarrow B_5H_9 + H_2$	$B_6H_{12} \rightarrow B_5H_9 + BH_3$	$B_6H_{12} \rightarrow B_6H_{10} + H_2$
ΔH(400 K)	16.9	38.3	36.0	7.7[b]	−7.8	13.8	−3.9
ΔH^*(400 K)	26.8	40.5	39[c]		52.8	26[d]	37.4
A factor, s^{-1}	2×10^{13}				3×10^{13}		2×10^{13}

[a] The B_4H_8 molecule is the C_s structure (double-bridged). The barrier has been reduced by 6.6 kcal/mol which is the triple-bridged (C_1) and double-bridged (C_s) separation at the MP2/6-31G*//6-31G* level. [b] Calculated heat of reaction as written. The observed activation barrier for the first-order decomposition of B_5H_{11} is 17.4 and 14 kcal/mol when the rate data are replotted as a second-order reaction. [c] The activation barrier is estimated by adding the activation barrier for the reaction $BH_3 + B_3H_7 \rightarrow B_4H_{10}$ (3 kcal/mol) to the heat of reaction. [d] The activation barrier is estimated by adding the activation barrier for the reaction $BH_3 + B_2H_6 \rightarrow B_3H_9$ (15 kcal/mol) to the heat of reaction. [e] Experimental $\Delta H^* = 23.8 \pm 0.8$; experimental $A = 6 \times 10^{11}$ s^{-1}. [f] Experimental $\Delta H^* = 17.4 \pm 0.6$; experimental $A = 1.6 \times 10^7$ s^{-1}. [g] Experimental $\Delta H^* = 17.9 \pm 1.4$; experimental $A = 3.8 \times 10^7$ s^{-1}.

state, respectively. Single-point calculations at the MP2/6-31G* level are closer in energy, and at the MP4/6-31G*//6-31G* level the asymmetric transition is actually lower in energy than the symmetrical transition state.

The product (**1**) of asymmetrical elimination of H_2 from B_4H_{10} would contain a boron that has a low coordination due to the loss of a terminal *and* bridging hydrogen (**1**). An exhaustive search was made for the asymmetric transition state leading to **1**.

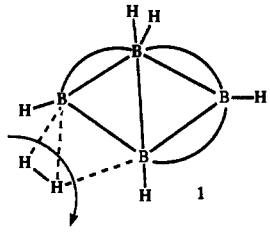

However, despite repeated attempts a stationary point could not be located. The B_4H_8 species which would result from asymmetric elimination was found to rearrange to **2** (MP2/6-31G* optimization), which is 9.4 kcal/mol higher in energy than the global minimum (a C_1 triple-bridged structure) at the [MP4/6-311G**//MP2/6-31G*] level (Table III). At the same level the *transition state* for symmetrical elimination of H_2 is 14.1 kcal/mol higher than the triple-bridged C_1 structure (Table III). Unless H_2 adds to **2** with a barrier of less than 4.7 kcal/mol, the asymmetric elimination of H_2 from B_4H_{10} will not be competitive with the symmetrical pathway.

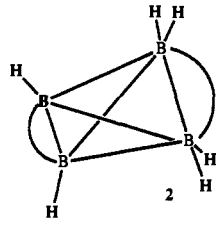

Three double-bridged structures (one of C_s symmetry, C_2 symmetry, and C_{2v} symmetry), a triple-bridged structure, and a quadruple-bridged structure of B_4H_8 were studied at all levels of theory (Table VII). The triple-bridged structure, which was identified as the lowest energy structure in an earlier study,[35] was reoptimized at the HF/3-21G level and was found to collapse to the double-bridged species. The identification as a minimum at the HF/3-21G level in the earlier work was due to incomplete geometry optimization. At the HF/6-31G* level the C_s symmetry double-bridged structure is slightly more stable than the triple-bridged structure. At all other levels the triple-bridged structure is more stable. Two double-bridged structures and the quadruple-bridged structure have nearly equal stability at correlated levels; however, at the Hartree–Fock level (6-31G*) the stability of the quadruple-bridged structure is significantly underestimated. In fact, the vibrational frequencies of the quadruple-bridged B_4H_8 structure at the HF/3-21G and HF/6-31G* levels reveal three

VII. Comparison of Relative Energies of B_4H_8 Isomers at Different Levels of Theory

	double-bridged			triple bridged	quadruple bridged
	C_s	C_2	C_{2v}		
6-31G*//6-31G*	−0.9	3.6	14.9	0.0	10.1
MP2/6-31G*//6-31G*	6.6	3.6	9.8	0.0	6.6
MP4/6-31G*//6-31G*	5.7	3.2	10.6	0.0	6.8
MP4/6-31G*//6-31G*+ZPC	5.0	2.9	10.8	0.0	4.2
MP2/6-31G*//MP2/6-31G*	5.6	4.6	9.0	0.0	6.9
MP4/6-31G*//MP2/6-31G*	4.9	4.0	9.9	0.0	7.1
MP2/6-311G**//MP2/6-31G*	5.4	4.9	8.5	0.0	6.0
[MP4/6-311G**]//MP2/6-31G*	4.7	4.3	9.4	0.0	6.2
[MP4/6-311G**]//MP2/6-31G*+ZPC	4.0	4.0	9.6	0.0	3.6

imaginary frequencies, which indicates the existence of at least one structure of lower energy. At the [MP4/6-311G**]//MP2/6-31G* level the triple-bridged structure is 4.0 kcal/mol more stable than both double-bridged structures and 3.6 kcal/mol more stable than the quadruple-bridged structure.

An analysis was made of the geometries of B_4H_8 structures optimized at different levels of theory (HF/3-21G, HF/6-31G*, MP2/6-31G*). In general, the bridging hydrogens become more symmetrical and the molecule becomes more compact (i.e. the B–B distances shorten). The double-bridged and quadruple-bridged structures show the strongest dependence on the level of theory used for geometry optimization (Table V). In the double-bridged structure, the bridging hydrogens shorten 0.10 Å to the bridgehead boron while the remaining bridging distances lengthen 0.08 Å as the level of theory improves from HF/3-21G to MP2/6-31G*. The transannular B–B distance and the average perimeter B–B distance contract 0.05 and 0.06 Å, respectively. In the quadruple-bridged structure, the bridging distances opposite the bridgehead borons decrease 0.10 Å as the level of theory improves (HF/3-21G → MP2/6-31G*) while the perimeter B–B distances decrease 0.04 Å. An analogous contraction of the B–B distance is observed in the C_{3v} symmetry structure of B_3H_9. The B–B distance is 2.168 Å at the SCF level with a (321/21) basis and decreases to 2.018 Å when electron correlation is introduced at the MP2 level in the same basis set.[23]

Locating the transition state for elimination of BH_3 from B_3H_9 required the use of a correlated wave function due to the underestimation of the stability of the three-center bond at the Hartree–Fock level.[14] A transition-state model with optimization at the HF/3-21G level has been reported for the elimination of BH_3 from B_3H_9 and from B_4H_8 in which a breaking and forming H···B interaction is constrained to be 1.7 Å.[36,38] The transition-state model for elimination of BH_3 from B_4H_{10} was 15.1 kcal/mol above products at the HF/3-21G level, but 0.9 kcal/mol below products ($BH_3 + B_3H_7$) at the MP2/6-31G* level. Clearly, electron correlation must be included in order to locate the

(35) McKee, M. L.; Lipscomb, W. N. *Inorg. Chem.* **1982**, *21*, 2846.

(36) Lipscomb, W. N. *Pure Appl. Chem.* **1983**, *55*, 1431.
(37) Ortiz, J. V.; Lipscomb, W. N. *Chem. Phys. Lett.* **1983**, *103*, 59.
(38) McKee, M. L. *Inorg. Chem.* **1986**, *25*, 3545–3547.

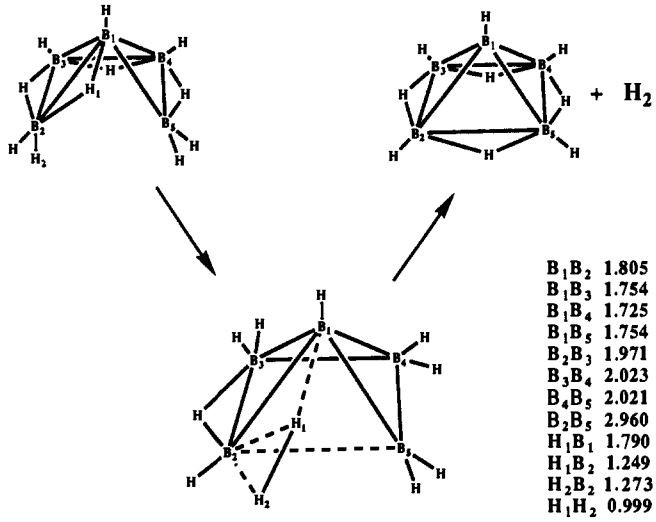

Figure 2. Selected geometric parameters of the transition state $B_5H_{11} \rightarrow B_5H_9 + H_2$ optimized at the HF/3-21G level. A bridging and terminal hydrogen (H_1 and H_2) become the hydrogen molecule.

transition state. The search was time consuming since the transition state has no elements of symmetry. The geometry, which is given in Figure 1, is characterized by a triple-bridged hydrogen where the three bridging distances are 1.495, 1.419, and 1.377 Å. The transition state for elimination of BH_3 from B_3H_9 was recently located[14] at a similar level of theory (polarization functions were added to all hydrogens as well as borons) where the corresponding bridging distances are 1.409, 1.329, and 1.533 Å. It is possible that these distances are unusually sensitive to the presence of polarization functions on the triple-bridged hydrogen since it is in a rather unique environment.

The transition state was not confirmed due to the large amount of computer time a frequency calculation at the MP2/6-31G* level would require. However, the identification as such is likely since all $3n - 6$ geometric parameters were optimized and the approximate Hessian matrix generated from the geometry searching routine indicated only one negative eigenvalue. In addition, if the stationary point were a second-order stationary point, the true transition state could *at most* be only 5.0 kcal/mol lower in energy since that is the energy difference between the stationary point and products, $B_3H_7 + BH_3$.

At the MP2/6-31G*//MP2/6-31G* level of theory, BH_3 elimination has a forward activation barrier of 45.9 kcal/mol and a reverse barrier of 5.0 kcal/mol. At the [MP4/6-311G**]+ZPC level, the barriers are reduced to 38.0 and 2.9 kcal/mol, respectively. Heat capacity corrections (to 400 K) increase the forward barrier to 40.5 kcal/mol and decrease the reverse barrier to 2.2 kcal/mol. These activation barriers are within 3 kcal/mol of those estimated from the constrained transition-state model.[36,38]

Elimination of H_2 from B_5H_{11} and B_6H_{12}. The decompositions of B_5H_{11} and B_6H_{12} have been studied in the gas phase.[5,6,8] For both boron hydrides the proposed slow step is the elimination of BH_3 (eqs 2b and 3b) rather than the elimination of H_2 (eqs 2a and 2b). In contrast, the decomposition of B_4H_{10} is believed to involve the elimination of H_2 rather than BH_3. To determine the nature of the higher barriers to H_2 elimination, the transition states were located at the HF/3-21G level for B_5H_{11} and B_6H_{12} (Figures 2 and 3). Since this level of theory (HF/3-21G) does not include polarization functions or electron correlation, the resulting geometries will be less accurate than MP2/6-31G* geometries determined for the smaller boron hydrides.

Minimum-energy structures for B_5H_{11}[21] and B_6H_{12}[22] have been reported previously. The transition state for $B_5H_{11} \rightarrow B_5H_9 + H_2$ involves the conversion of one terminal and one bridging hydrogen into molecular hydrogen. The H–H distance (0.999 Å) is longer than the H–H distance in the 3-21G transition state for symmetric elimination of H_2 in B_4H_{10} (0.760 Å), indicating an earlier transition state. The barrier at the MP2/6-31G*//3-21G+ZPC level is 51.8 kcal/mol for the forward barrier and

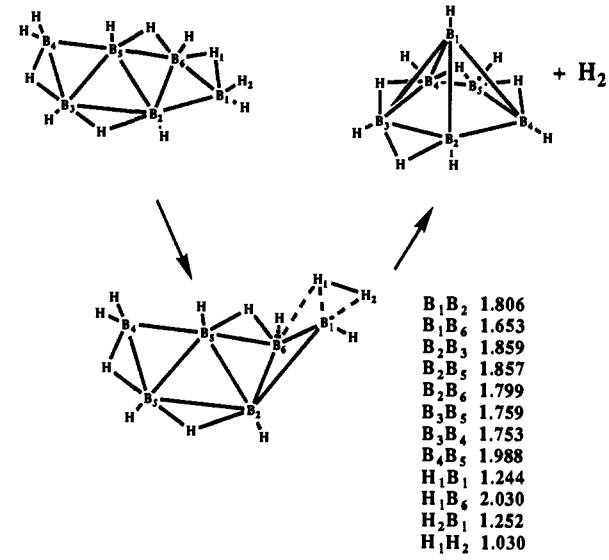

Figure 3. Selected geometric parameters of the transition state $B_6H_{12} \rightarrow B_6H_{10} + H_2$ optimized at the HF/3-21G level. The distances B_3B_5 and B_2B_5 elongate while B_1 approaches B_3, B_4, and B_5.

62.1 kcal/mol for the reverse barrier (at 400 K, 52.8 and 60.6 kcal/mol, respectively). The forward barrier is over 15 kcal/mol higher than that for elimination of H_2 in B_4H_{10} at the same level. The observed decomposition of B_5H_{11} occurs with a much lower activation barrier of 17.4 kcal/mol,[5] which indicates that H_2 elimination does not occur when B_5H_{11} decomposes.

Elimination of H_2 from B_6H_{12} also occurs by the conversion of a terminal and bridging hydrogen into molecular hydrogen. The H–H distance of 1.030 Å in the transition state is similar to the corresponding distance in the B_5H_{11} transition state. To form $B_6H_{10} + H_2$ from the transition state, the B_3B_5 and B_2B_5 distances must increase and the B_1B_5, B_1B_3, and B_1B_4 distances must decrease (Figure 3). In addition, one terminal hydrogen must become bridging between B_4 and B_5. The activation barrier is 37.1 kcal/mol at the MP2/6-31G*//3-21G+ZPC level (37.4 kcal/mol at 400 K), which is 14.7 kcal/mol lower than the analogous barrier in B_5H_{11}. However, the observed barrier for decomposition of B_6H_{12} (17.9 kcal/mol[8]) indicates that the H_2 elimination pathway is not competitive.

Elimination of BH_3 from B_5H_{11} and B_6H_{12}. The proposed slow step in the decomposition of B_5H_{11} and B_6H_{12} is elimination of BH_3 (eqs 2b and 3b). All efforts to locate the transition state at the Hartree–Fock level failed. A characteristic feature of these transition states appears to be a triple-bridged hydrogen, which is found in the transition state for elimination of BH_3 from B_3H_9 and B_4H_{10} where it was necessary to include electron correlation when locating these transition states. The transition state for elimination of BH_3 from B_3H_9 was located with a [3s2pld]/[2slp] basis set on boron and hydrogen and including electron correlation at the MP2 level.[14] Energy differences were evaluated at the CCSD+T(CCSD) level employing a slightly larger basis set ([4s3pld]/[3slp]). The barrier (including zero-point correction) for $B_3H_9 \rightarrow B_2H_6 + BH_3$ was 18.4 kcal/mol (18.8 kcal/mol at 400 K). In comparison, the transition state for $B_4H_{10} \rightarrow B_3H_7 + BH_3$, located at the MP2/6-31G* level and single-point at the [MP4/6-311G**]+ZPC level, was 38.0 kcal/mol (40.5 kcal/mol at 400 K). If the reverse reactions are considered, the reaction $B_2H_6 + BH_3 \rightarrow B_3H_9$ may be taken as an example of BH_3 adding to a boron hydride with a high barrier (14.9 kcal/mol) while the reaction $B_3H_7 + BH_3 \rightarrow B_4H_{10}$ is an example of BH_3 adding to a boron hydride with a low barrier (2.9 kcal/mol). As a rough guide we can estimate that BH_3 will add to a boron hydride with an activation barrier between 3 and 15 kcal/mol. The high activation barrier will be more likely for addition to a stable boron hydride as B_2H_6 or B_5H_9 while the low barrier will be more likely for addition to a reactive boron hydride as B_3H_7 or B_4H_8.

Since addition of BH_3 to B_4H_8 is an example of addition of BH_3 to a reactive boron hydride, an estimate of the barrier of reaction

2b can be made by adding 3 kcal/mol (estimate of the reverse reaction) to the heat of reaction. Likewise, an estimate of the barrier of reaction for eq 3b can be made by adding 15 kcal/mol (addition of BH_3 to B_5H_9, a stable boron hydride) to the heat of reaction. Heats of reaction can be calculated more reliably and therefore an estimate of the reaction barrier for eqs 2b and 3b can be made.

The heat of reaction at the MP2/6-31G*//3-21G+ZPC level for the reaction $B_5H_{11} \rightarrow B_4H_8 + BH_3$ is 32.7 kcal/mol (36.0 kcal/mol at 400 K). The estimated barrier for the reaction is therefore about 39 kcal/mol, which is the heat of reaction (36 kcal/mol) plus the reverse barrier for addition of BH_3 to a reactive boron hydride, B_4H_8 (3 kcal/mol).

For the decomposition of B_5H_{11}, the estimated barrier for the reaction $B_5H_{11} \rightarrow B_4H_8 + BH_3$ is substantially greater than that observed for decomposition of B_5H_{11} (39 (estimated) and 17.4 kcal/mol (exptl)[5]). It would appear that either the estimated barrier is in error by over 20 kcal/mol or B_5H_{11} decomposes by a different mechanism. Considering the possible errors in the estimation for the reverse activation barrier and errors in the level of theory for determining the heat of reaction, the uncertainty is probably about ±10 kcal/mol. The lower limit of 29 kcal/mol would still indicate that direct decomposition to $B_4H_8 + BH_3$ is not involved. Formation of B_4H_8 catalytically could not explain the discrepancy since the barrier can only be reduced by a maximum of 3 kcal/mol.

An alternative explanation is that the reaction proceeds by a bimolecular rate-determining step (eq 15). The strongest evidence for a bimolecular mechanism is the pre-exponential factor for the decomposition of B_5H_{11} (1.6×10^7 s^{-1}), which is about 10000 times smaller than the low end of unimolecular pre-exponential factors[39] (10^{11}–10^{15} s^{-1}). Alternatively, eq 15 could represent a pre-equilibrium step followed by a rate-determining step. Although an effort was made, a reasonable series of steps consistent with the known[5,6] kinetics of decomposition of B_5H_{11} could not be found.

$$2B_5H_{11} \rightarrow B_3H_7 + B_5H_9 + B_2H_6 \qquad (15)$$

If the rate data for decomposition of B_5H_{11} from ref 5 is plotted as a second-order reaction, the activation barrier is about 14 kcal/mol, which can be compared to a calculated endothermicity of 7.7 kcal/mol for eq 15.

The decomposition of B_6H_{12} via eq 3b is estimated to proceed with a barrier of 29 kcal/mol (15 kcal/mol reverse barrier for addition of BH_3 to a stable boron hydride and 14 kcal/mol endothermicity of the forward reaction), which is 11 kcal/mol greater than the observed barrier of 17.9 kcal/mol.[8] While the observed barrier is nearly within the 10 kcal/mol uncertainity estimated for the barrier of $B_6H_{12} \rightarrow B_5H_9 + BH_3$, it is possible that B_6H_{12} also decomposes with a mechanism similar to B_5H_{11} since the pre-exponential factor for the observed[8] decomposition of B_6H_{12} (3.8×10^7 s^{-1}) is very similar to the observed pre-exponential factor for the decomposition of B_5H_{11} (1.6×10^7 s^{-1}).

(39) Benson, S. W. *Thermochemical Kinetics*; J. W. Wiley and Sons: New York, 1976.

Conclusion

Several reactions of possible significance to pyrolysis of diborane were studied. Two pathways of B_4H_{10} decomposition were considered, elimination of H_2 to form B_4H_8 and production of BH_3 plus B_3H_7. In agreement with experiment, the favored pathway was found to be elimination of H_2 with an activation barrier of 26.8 kcal/mol.

Four isomers of B_4H_8 were optimized at the MP2/6-31G* level, the double-, triple-, and quadruple-bridged isomers. At the [MP4/6-311G**]+ZPC level, the triple-bridged isomer was found to 4.0 kcal/mol more stable than the double-bridged isomer.

Decomposition of B_5H_{11} and B_6H_{12} by H_2 elimination is found to be inhibited due to high activation barriers. The experimental decomposition of B_5H_{11} is predicted not to occur by a unimolecular pathway to $B_4H_8 + BH_3$ due to an excessively high heat of reaction for formation of unimolecular products. The first step of an alternative mechanism is suggested which involves two B_5H_{11} molecules forming B_3H_7, B_5H_9, and B_2H_6. This alternative mechanism is supported by an experimental pre-exponential factor that is in the range of bimolecular reactions.

Acknowledgment. We thank the donors of the Petroleum Research Fund, administered by the American Chemical Society, for financial support. Computer time for this study was made available by the Auburn University Computer Center, the Alabama Supercomputer Network, and the NSF-supported Pittsburgh Supercomputer Center. We thank the IBM Corp. for access to an IBM 3090 computer at the Los Angeles Scientific Center under Grant RSP 1039. I also acknowledge Dr. W. N. Lipscomb in whose laboratory this work was started.

Supplementary Material Available: The computer-generated coordinates (Z matrix) of small boron hydrides optimized at the MP2/6-31G* level and the $B_5H_{11} \rightarrow B_5H_9 + H_2$ and $B_6H_{12} \rightarrow B_6H_{10} + H_2$ transition states optimized at the HF/3-21G level (5 pages). Ordering information is given on any current masthead page.

Electrocyclic Ring Openings of Dialkylcyclobutenes: Anomalies Explained

E. Adam Kallel, Ying Wang, David C. Spellmeyer, and K. N. Houk*

Contribution from the Department of Chemistry and Biochemistry, University of California, Los Angeles, California 90024-1569. *Received December 22, 1989*

Abstract: The electrocyclic reactions of dialkylcyclobutenes were examined with use of ab initio molecular orbital theory. *cis*-3,4-Dimethylcyclobutene possesses a destabilizing steric interaction that elevates the energy of the ground state and leads to a faster rate of reaction than expected on the basis of methyl groups effects in other systems. The ring openings of 3-alkyl-3-methylcyclobutenes were shown by Curry and Stevens to involve inward rotation of the larger group in some cases. Calculations on 3-ethyl-3-methylcyclobutene show that the product distribution can be explained as a result of more favorable gauche interactions upon inward rotation of the larger ethyl group. An extremely large stereochemical dependence of torsional barriers of alkyl groups is revealed in these calculations.

Introduction

During the last 5 years the stereoselectivities of cyclobutene ring openings have been studied intensively from both the theoretical and experimental points of view.[1-4] In the original derivation of substituent effects upon outward or inward conrotation of substituents in the electrocyclization of cyclobutenes, additivity

(1) Carpenter, B. *Tetrahedron* **1978**, *34*, 1977.

0002-7863/90/1512-6759$02.50/0